Supplemental Material

Post-transcriptional regulation of IFI16 promotes inflammatory endothelial pathophenotypes observed in pulmonary arterial hypertension

Rashmi J. Rao[a, #], Jimin Yang[b, #], Siyi Jiang[a], Wadih El-Khoury[a], Neha Hafeez[a,c], Satoshi Okawa[a,d,e], Yi Yin Tai[a], Ying Tang[a], Yassmin Al Aaraj[a], John Sembrat[f], Stephen Y. Chan[a]

a) Center for Pulmonary Vascular Biology and Medicine, Pittsburgh Heart, Lung, Blood, and Vascular Medicine Institute, Division of Cardiology, Department of Medicine, University of Pittsburgh School of Medicine and University of Pittsburgh Medical Center, Pittsburgh, PA, USA
b) Department of Molecular Biology, Jeonbuk National University, Jeonju, South Korea
c) Department of Medicine, Hospital of the University of Pennsylvania, Philadelphia, PA, USA
d) Department of Computational and Systems Biology, University of Pittsburgh School of Medicine and University of Pittsburgh Medical Center, Pittsburgh, PA, USA
e) McGowan Institute for Regenerative Medicine, University of Pittsburgh School of Medicine and University of Pittsburgh Medical Center, Pittsburgh, PA, USA
f) Division of Pulmonary, Allergy, Critical Care, and Sleep Medicine, Department of Medicine, University of Pittsburgh School of Medicine, Pittsburgh, PA, USA

[*#] Equal Contribution

Table S1. Clinical Characteristics for Group 1 PAH Patients (Human Lung Tissue)

Group	Age	Gender	mPAP
Control 1	36	M	-
Control 2	37	M	-
Control 3	66	M	-
Control 4	13	M	-
Control 5	44	F	-
PH 1: Connective tissue disease	53	F	53
PH 2: IPAH	21	M	69
PH 3: IPAH	50	F	56
PH 4: IPAH	51	F	59

Table S2. Clinical Characteristics for Group 1 PAH Patients (Human Blood Samples)

Group	Age	Gender	mPAP
Control 1: No PH	58	M	14
Control 2: No PH	61	F	8
Control 3: Healthy control	40	F	-
Control 4: Healthy control	66	F	-
Control 5: Healthy control	53	F	-
PH 1: IPAH	64	M	53
PH 2: IPAH	66	F	46
PH 3: Connective tissue disease	62	F	22
PH 4: IPAH	40	F	42
PH 5: IPAH	67	M	56
PH 6: IPAH	63	M	59
PH 7: IPAH	72	M	24
PH 8: IPAH	54	F	44

Table S3. Silencer RNA Reagent Information (Thermo Fisher Scientific)

Reagent	Catalog #
Negative control siRNA (#1)	ON-TARGETplus Non-targeting siRNA(D-001810-01-05)
IFI16 siRNA	ON-TARGETplus Human WTAP siRNA (LQ-017323-00-0002)
WTAP siRNA (siRNA #1)	ON-TARGETplus Human IFI16 siRNA (LQ-020004-00-0002)
BMPR2 siRNA	ON-TARGETplus BMPR2 siRNA (LQ-005309-00-0005)
Negative control siRNA (#2)	Silencer AM4611
WTAP siRNA (siRNA #2)	Silencer ID: 44219

Table S4. TaqMan Primers Reagent Information (Thermo Fisher Scientific)

Reagent	Catalog #
IFI16	Hs04987070_m1
WTAP	Hs00986757_m1

VCAM1	Hs01003372_m1
ICAM1	Hs01109748_m1
IL6	Hs00174131_m1
NF-κB	Hs00765730_m1
IL-1β	Hs01555410_m1
GAPDH	Hs02786624_g1
ACTB	Hs1060665_g1
Mouse *WTAP*	Mm05666501_g1
Mouse *ACTB*	Mm02619580_g1

Table S5. Antibody Reagent Information

Company	Use	Reagent	Catalog #
Proteintech	Western blot	WTAP	60188-1-Ig
Santa Cruz	Western blot	ACTB	sc-47778
Santa Cruz	Immunofluorescence	WTAP	sc-374280
ThermoFisher	Immunofluorescence	IFI16	PA5120684
Abcam	Immunofluorescence	vWF	ab287962
ThermoFisher	Immunofluorescence	vWF	MA5-14029

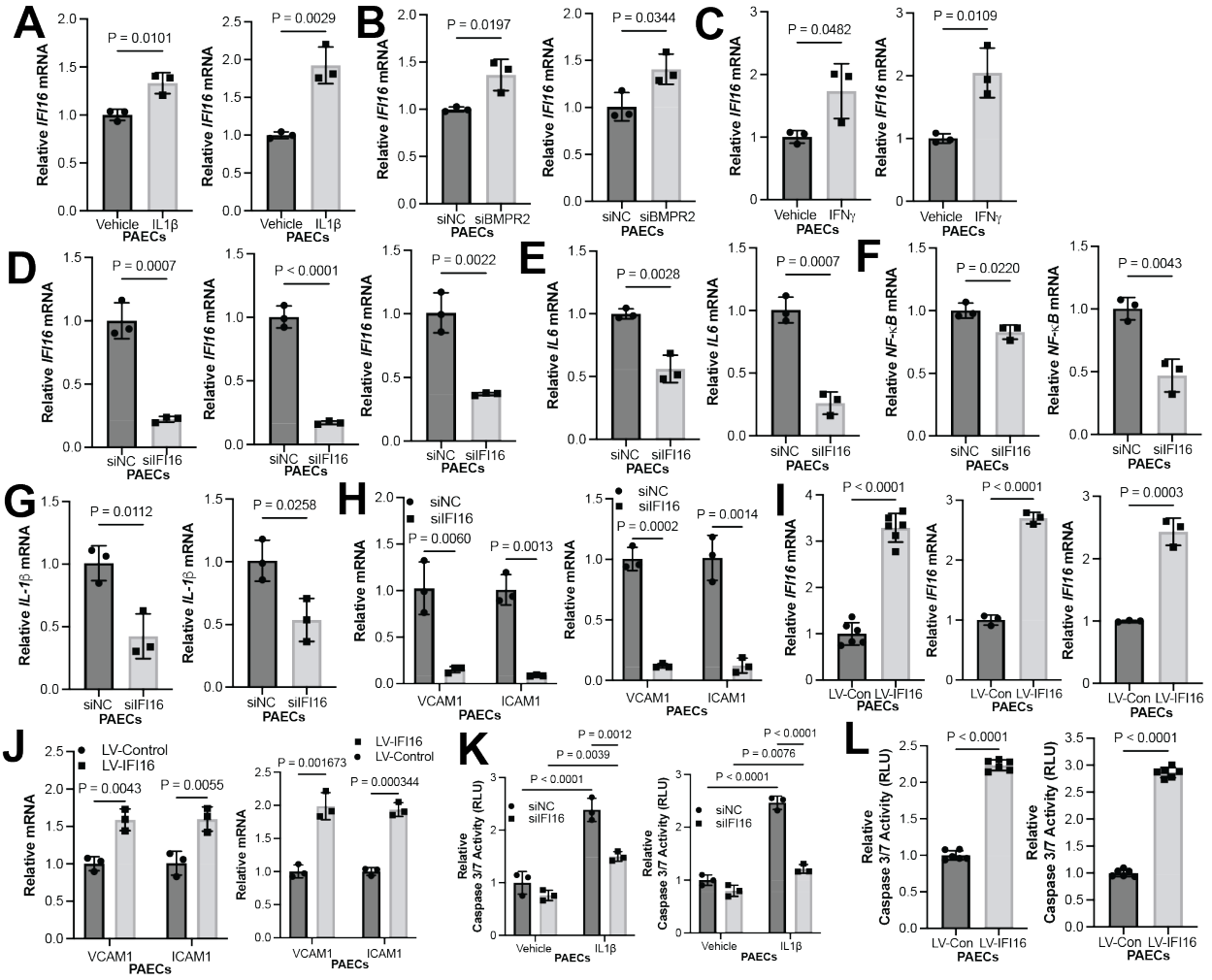

Figure S1. Inflammatory and genetic regulation of endothelial IFI16 expression.

(**A**) Experimental repeats of Fig. 1B. By RT-PCR, relative IFI16 expression (n=3/group) was measured in IL-1β-treated (2 ng/mL) vs. vehicle control (0 ng/mL) PAECs (n=3/group). (**B**) Experimental repeats of Fig. 1C. By RT-PCR, relative IFI16 expression was measured following siRNA-mediated BMPR2 knockdown (siBMPR2) vs. control (siNC) PAECs (n=3/group). (**C**) Experimental repeats of Fig. 1D. By RT-PCR, relative IFI16 expression was measured in IFNγ-treated vs. vehicle control PAECs (n=3/group). (**D**) By RT-PCR, relative IFI16 expression was measured in IFI16-deficient (siIFI16) vs. control (siNC) PAECs (n=3/group). Experimental repeats of Fig. 1E-G. By RT-PCR, relative expression was of inflammatory cytokines (**E**) IL-6, (**F**) NF-KB, and (**G**) IL-1β were measured in IFI16-deficient (siIFI16) vs. control (siNC) PAECs (n=3/group).

(**H**) Experimental repeats of Fig. 1H. By RT-PCR, relative expression was measured of endothelial inflammatory markers VCAM1 and ICAM1 in IFI16-deficient (siIFI16) vs. control (siNC) PAECs (n=3/group); (**I**) By RT-PCR, relative IFI16 expression was measured following IFI16 overexpression (LV-IFI16) vs. control (LV-Control) PAECs (n=6 or 3/group). (**J**) Experimental repeats of Fig. 1I. Relative expression of VCAM1 and ICAM1 was measured following overexpression (LV-IFI16) vs. control (LV-Con) transduction IFI16 in PAECs (n=3/group). (**K**) Experimental repeats of Fig. 1J. Relative caspase 3/7 activity was measured after IFI16 knockdown (siIFI16) vs. control in PAECs +/- IL-1β (n=3/group). (**L**) Experimental repeats of Fig. 1K. Relative caspase 3/7 activity was measured following IFI16 overexpression (LV-IFI16) vs. control (LV-Con) transduction in PAECs (n=6/group). In (**A-L**), mean expression in control groups was assigned a fold change of 1, to which relevant samples were compared. P-values calculated by two-tailed Student's *t* test (**A-J, L**), and two-way ANOVA and post-hoc Bonferroni test (**K**), presented as mean +/- SEM.

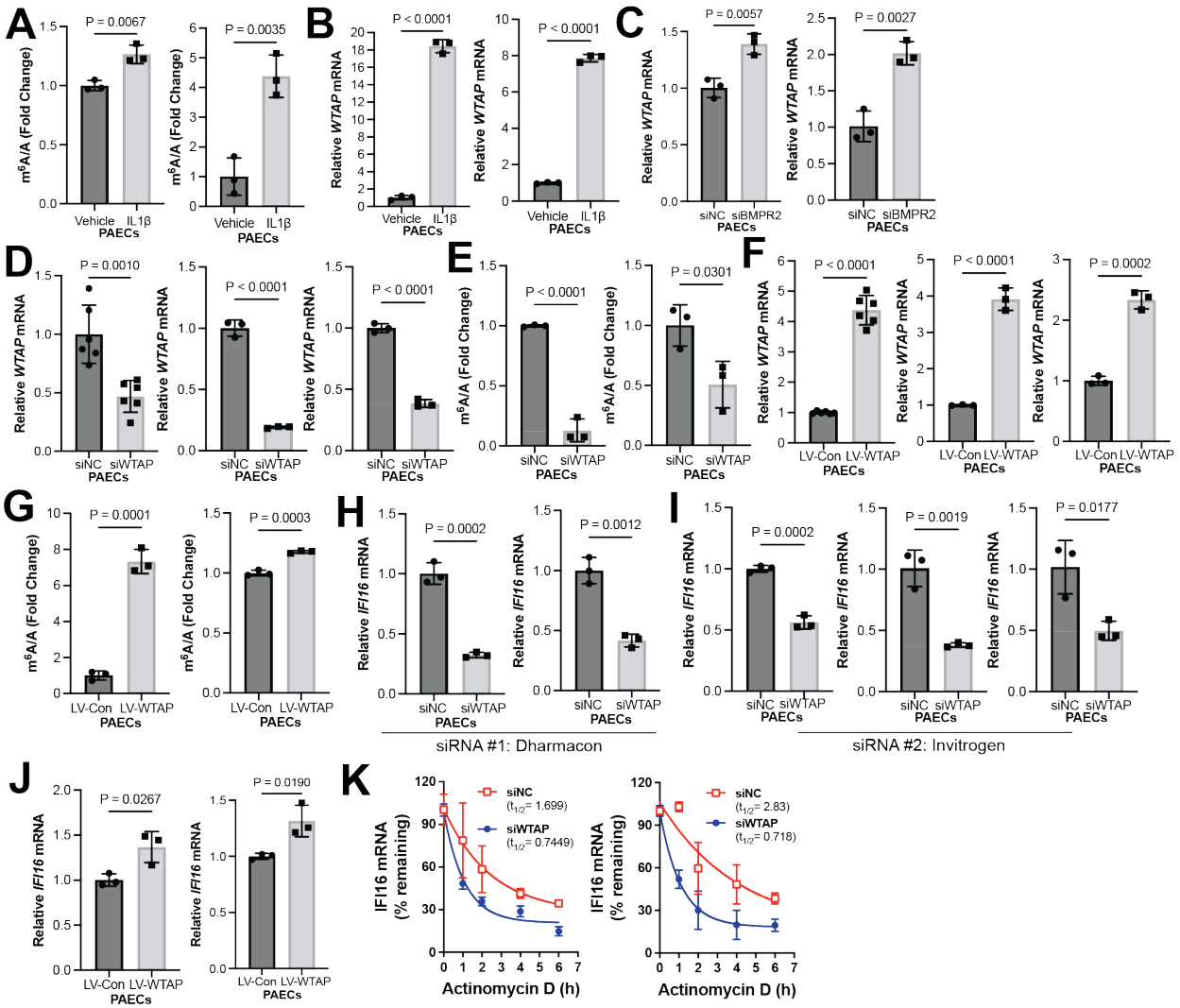

Figure S2. Inflammatory and genetic regulation of endothelial WTAP expression. (**A**) Experimental repeats of Fig. 2B. Fold change of m6A/A was measured by colorimetric assay in IL-1β-treated vs. control (vehicle) PAECs (n=3/group). (**B**) Experimental repeats of Fig. 2D. By RT-PCR, relative WTAP transcript expression was measured (n=3/group) in IL-1β-treated (2 ng/mL) vs. vehicle control (0 ng/mL) PAECs (n=3/group). (**C**) Experimental repeats of Fig. 2E. By RT-PCR, relative WTAP expression was measured following siRNA-mediated BMPR2 knockdown (siBMPR2) vs. control (siNC) PAECs (n=3/group). (**D**) By RT-PCR, relative WTAP expression was measured in WTAP-deficient (siWTAP) vs. control (siNC) PAECs (n=6 or

3/group). (**E**) Experimental repeats of Fig. 2F. Fold change of m6A/A was measured by colorimetric assay in WTAP-deficient (siWTAP) vs. control (siNC) PAECs (n=3/group). (**F**) By RT-PCR, relative WTAP expression was measured following WTAP overexpression vs. control PAECs (n=6 or 3/group). (**G**) Experimental repeats of Fig. 2G. Fold change of m6A/A was measured by colorimetric assay following WTAP overexpression (LV-WTAP) vs. control (LV-Con) PAECs (n=3/group). (**H**) Experimental repeats of Fig. 2H. By RT-PCR, relative IFI16 expression was measured in WTAP-deficient (siWTAP) vs. control (siNC) PAECs (n=3/group) using siRNA #1 (Dharmacon). (**I**) By RT-PCR, relative IFI16 expression was measured in WTAP-deficient (siWTAP) vs. control (siNC) PAECs (n=3/group) using siRNA #2 (Invitrogen). (**J**) Experimental repeats of Fig. 2I. By RT-PCR, relative IFI16 expression was measured after WTAP overexpression (LV-WTAP) vs. control (LV-Con) transduction in PAECs (n=3/group). (**K**) Experimental repeats of Fig. 2K. IFI16 mRNA decay was measured in WTAP-deficient (siWTAP) vs. control (siNC) PAECs following inhibition of cellular transcription by actinomycin D (n=3/group, presented as mean and 95% CI). In (**A-J**), mean expression in control groups was assigned a fold change of 1, to which relevant samples were compared. P-values calculated by two-tailed Student's *t* test (**A-J**) presented as mean +/- SEM.

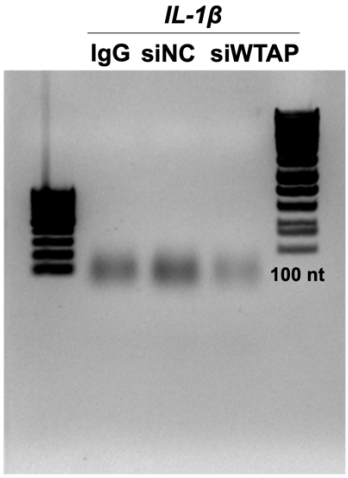

Figure S3. Fragmentation of RNA for MeRIP. Calibration of RNA fragmentation and validation of size distribution are shown by gel electrophoresis prior to immunoprecipitation by MeRIP. Fragments converged on ~100 nucleotides in size.

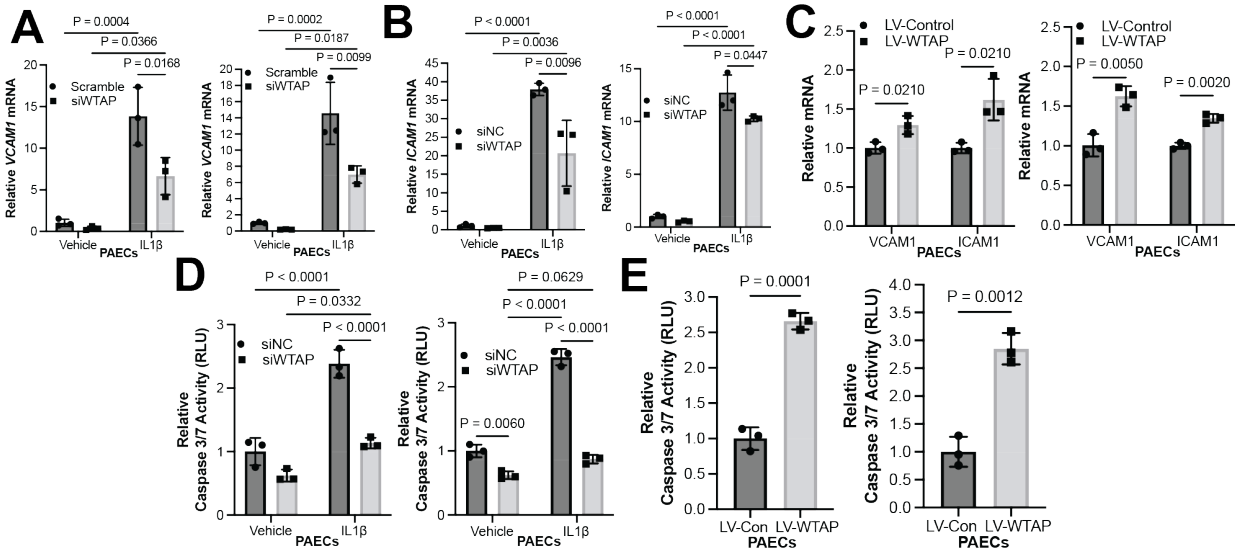

Figure S4. WTAP phenocopies IFI16-driven endothelial pathophenotypes in PAECs. (**A-B**) Experimental repeats of Fig. 3A-B. By RT-PCR, relative expression was measured of endothelial inflammatory markers (**A**) VCAM1 and (**B**) ICAM1 in WTAP-deficient (siWTAP) vs. control (siNC) with and without IL-1β in PAECs (n=3/group). (**C**) Experimental repeats of Fig. 3C. Relative expression of VCAM1 and ICAM1 was measured following WTAP overexpression (LV-WTAP) vs. control (LV-Con) transduction in PAECs (n=3/group). (**D**) Experimental repeats of Fig. 3D. Relative caspase 3/7 activity was measured after WTAP knockdown (siWTAP) vs. control in PAECs with and without IL-1β (n=3/group). (**E**) Experimental repeats of Fig. 3E. Relative caspase 3/7 activity was measured after WTAP overexpression (LV-WTAP) vs. control (LV-Con) transduction in PAECs (n=3/group). In all panels, mean expression in control groups was assigned a fold change of 1, to which relevant samples were compared. P-values calculated by two-tailed Student's *t* test (**C, E**) and two-way ANOVA and post-hoc Bonferroni test (**A, B, D**), presented as mean +/- SEM.